ANTIOXIDANTS & REDOX SIGNALING
Volume 8, Numbers 5 & 6, 2006

Forum Original Research Communication

Development of the Adductome Approach to Detect DNA Damage in Humans

ROBERT A. KANALY,[1] TOMOYUKI HANAOKA,[2] HARUHIKO SUGIMURA,[3] HIROKAZU TODA,[1] SABURO MATSUI,[1] and TOMONARI MATSUDA[1]

ABSTRACT

The development of new strategies designed to detect DNA damage caused by oxidative stress and other means may advance our understanding of the roles of such types of damage in the etiology of cancers, in aging processes, and as biomarkers of exposure. A DNA adduct detection method that uses liquid chromatography coupled with electrospray ionization tandem mass spectrometry (LC/ESI–MS/MS) to detect multiple DNA adducts in human lung tissue is reported herein. This adductome analysis strategy is designed to detect the neutral loss of 2′-deoxyribose from positively ionized 2′-deoxynucleoside adducts in multiple reaction ion monitoring mode (MRM) transmitting the $[M + H]^+ > [M + H - 116]^+$ transition over a total of 374 transitions in the mass range from *m/z* 228.8 to *m/z* 602.8. Data analysis is optimized and coupled with a comprehensive manual screening process designed to minimize the number of artifactual adducts appearing in the final analysis. In the final analysis, putative adducts were organized into an adductome map and unambiguous confirmation of selected oxidative adducts were made by stable isotope dilution and comparison to authentic standards. The future applications of this method are discussed. *Antioxid. Redox Signal.* 8, 993–1001.

INTRODUCTION

Cellular DNA is continuously vulnerable to modification by exposure to electrophilic molecules that originate from both exogenous and endogenous sources. Such DNA modifications result in the formation of adducted DNA that, if not repaired, may interfere with sequence translation and ultimately result in potentially deleterious modifications to gene expression. As such, DNA adducts are implicated in mutagenesis, carcinogenesis, and aging, and to understand more clearly their roles in the etiology of cancers and aging processes is of much interest.

Currently, there are wide gaps in our knowledge of DNA adducts, especially as pertains to interindividual and intertissue differences. At any point in time, the numbers, types, and abundances of DNA adducts present in the DNA of a particular tissue reflect a multitude of complex factors including metabolism, recent exposure, chronic exposure, repair processes, and the health status of the organism, for example. The dynamic nature of their existence is cause for the development of creative methods to analyze DNA adducts, and various strategies have been engineered for their detection, including the highly-sensitive ^{32}P-postlabeling technique, electromigration methods, and immunoassay (7). However, the advent of newer spectrometric methods are now enabling the scientific community to perform more powerful analyses. Liquid chromatography coupled with electrospray ionization tandem mass spectrometry (LC/ESI–MS/MS) has emerged as a useful technique that offers excellent sensitivity and selectivity. In addition to allowing for the measurement of DNA adducts with detection in the picogram range, 1 adduct per 10^7 to 10^9 bases (13), tandem MS also offers powerful selectivity options by utilizing two stages of mass analysis: one stage by which to preselect an ion of interest and a second by which to analyze the fragments induced. Recently, tandem MS methods have been developed for measuring different DNA adduct types, from different tissue types and from different organisms including from liver, lung, and pancreas of mice, rats, and humans (2, 5, 12, 14). A broader approach to simultaneously monitor multiple adduct types by quantitative

[1]Department of Technology and Ecology, Graduate School of Global Environmental Studies, Kyoto University, Kyoto, Japan.
[2]Epidemiology and Prevention Division, National Cancer Center Research Institute, Tokyo, Japan.
[3]Department of Pathology, Hamamatsu University School of Medicine, Hamamatsu, Japan.

LC/ESI–MS/MS was also undertaken whereby four oxidative lesions, 8-oxo-7,8-dihydro-2′-deoxyguanosine (8-oxo-dG), pyrimido[1,2α]purine-10(3H)one-2′-deoxy-guanosine (malonaldehyde-dG), and two etheno-adducts were measured in rat and human liver DNA (4). Additionally, measurement of multiple DNA adducts has been carried out by other means such as ^{32}P-postlabeling in human lung (8) and pancreas tissue (9), or by a combination of ^{32}P-postlabeling and the aldehyde reactive probe slot blot assay in multiple human tissues (1).

Until now, simultaneous monitoring of large numbers of DNA adduct types has been explored little due to technical constraints. The development of a methodology for multiple adduct detection that may eventually be coupled with adduct identification processes would expand our current limitations at analyzing multiple adducts. Advantages of such a methodology include the examination of differences between individuals, exposures, and tissue types on a larger scale. Herein, the adductome approach for the detection of multiple DNA adducts in human tissue is illustrated and the future applications of this technique are discussed. By approaching the issue of measuring DNA adducts from a comprehensive perspective, we expect that further insights shall be garnered by this approach that will complement the currently used approaches.

MATERIALS AND METHODS

Chemicals and biochemicals

[U-$^{15}N_5$]-2′-Deoxyguanosine ([U-$^{15}N_5$]-dG), 98% purity, was purchased from Cambridge Isotope Laboratories, Inc. (Andover, MA). The enzymes micrococcal nuclease (MN) and bovine spleen phosphodiesterase II (SPD) were purchased from Worthington Biochemical Corp. (Lakewood, NJ). Bacterial alkaline phosphatase Type III (*E. coli*) was from Sigma Co. (St. Louis, MO). The analytical standards of the DNA adducts, N^2-ethyl-2′-deoxyguanosine (N^2-ethyl-dG), N^2-methyl-2′-deoxyguanosine (N^2-methyl-dG), and the stereoisomers α-*S*- and α-*R*-methyl-γ-hydroxy-1,N^2-propano-2′-deoxyguanosine (1,N^2-PdG$_1$, 1,N^2-PdG$_2$) were synthesized as described below, while standards of 1,N^6-etheno-2′-deoxyadenosine (ϵdA), 8-oxo-dG, and dideoxyinosine (ddI) were purchased from Sigma. Acetaldehyde (AA), formaldehyde, *trans*-2-butenal (crotonaldehyde), sodium cyanoborohydride ($NaBH_3CN$), dimethyl sulfoxide (DMSO), and methanol, HPLC grade, were purchased from Wako Chemical (Osaka, Japan).

Preparation of stable isotope internal standards

[U-$^{15}N_5$]-N^2-Ethyl-dG was prepared using a modification of a previous method (15) as follows: 100 µl of AA was reacted with [U-$^{15}N_5$]-dG (1 mg/ml) in a 1.5 ml-volume reaction vessel (total reaction volume of 1 ml) at 37°C for 12 h. Afterwards, $NaBH_3CN$, approximately 20 mg, was added to the mixture in 30 min intervals over a period of 2 h while the reaction was continued at 37°C. The resulting solution was subjected to reverse phase column chromatography by application to Sep-Pak C18 cartridges (Waters Corp., Milford, MA) whereby the columns were preconditioned with 10 ml methanol and 5 ml distilled water, and the sample was applied and eluted with approximately 5 ml of methanol. After purification, the sample was vacuum-concentrated and redissolved in 200 µl of DMSO. Fifty microliter aliquots of sample were subjected to preparative HPLC using a Shimadzu LC10-ATVP model pump (Shimadzu, Kyoto, Japan) equipped with a Rheodyne model 7725i injector (Rheodyne, Cotati, CA) and a C18 reverse-phase column (Shim-pack FC-ODS, 150 × 4.6 mm, Shimadzu), and UV-positive fractions were collected by hand. The mobile phase consisted of a water and methanol gradient, whereby water was increased to 40% over a period of 40 min at a flow rate of 1 ml/min. [U-$^{15}N_5$]-1,N^2-PdG$_1$ and [U-$^{15}N_5$]-1,N^2-PdG$_2$ were prepared by adding 20 µl of crotonaldehyde to 1 ml of [U-$^{15}N_5$]-dG (1 mg/ml) for a reaction time of 12 h at 37°C. Purification of the diastereomers [U-$^{15}N_5$]-1,N^2-PdG$_1$ and [U-$^{15}N_5$]-1,N^2-PdG$_1$ was carried out in the same manner as described for the preparation of [U-$^{15}N_5$]-N^2-ethyl-dG. Unlabeled authentic standards of N^2-ethyl-dG, 1,N^2-PdG$_1$ and 1,N^2-PdG$_2$ were prepared in the same manner, but with unlabeled dG. N^2-methyl-dG was prepared in the same manner as N^2-ethyl-dG except that the starting material was formaldehyde rather than AA. Standard purity was confirmed by measuring absorbance in a GeneSpec V ultraviolet (UV)-visible spectrophotometer with accompanying software (Hitachi Naka Instruments, Co., Ltd., Tokyo, Japan) and the quantity of standard recovered was measured.

Lung tissue DNA extraction and digestion

Human lung tissue was obtained postmortem within 24 h after expiration and stored at −80°C. The subjects were two Japanese males aged 59 and 70 years, who were characterized as a smoker and nonsmoker, respectively. DNA was purified from lung tissue with the Puregene DNA Purification system (Gentra Systems, Minneapolis, MN) according to the manufacturer's instructions and resuspended in 500 µl of distilled water. DNA quantification was carried out by measuring the absorbance of the purified sample product at 260 and 280 nm in a 50-µl volume quartz cell by a UV-visible spectrophotometer. Based on the concentration of DNA in each sample solution, aliquots containing 100 µg of DNA were transferred to 1.5-ml Eppendorf tubes and the distilled water was removed by vacuum concentration in a CC-105 model centrifugal concentrator (Tomy Seiko Co., Tokyo, Japan). Following water removal, lung DNA samples were enzymatically hydrolyzed to their corresponding 2′-deoxyribonucleoside 3′-monophosphates by the addition of 100 µl of MN/SPD buffer (200 m*M* citrate buffer, 100 m*M* $CaCl_2$, pH 6.0), plus 10 µl each of MN (15 U/µl) and SPD (0.05 U/µl). Solutions were gently mixed by hand and incubated for 2 h at 37°C. After incubation, 30 units of alkaline phosphatase, 100 µl of 0.5 M Tris HCl (pH 8.5), 50 µl of 20 m*M* $ZnSO_4$ and 700 µl of distilled water were added. The solution was gently mixed and incubated further for 3 h at 37°C. After 3 h, the total sample volume was reduced to approximately 40 µl by centrifugal concentration and the tube contents were extracted twice with chilled methanol. To each tube, 300 µl of methanol was added and the tubes were shaken for approximately 3 min at 2,500 rpm on an Eyela model CM-100 mixer (Tokyo, Japan), followed by centrifugation at 15,000 *g* and 4°C for 5 min in a Tomy MTX-150 refrigerated centrifuge (Tomy Seiko Co.). The supernatant extract was removed to a new tube, and the

pellet was extracted again with methanol and combined with the previous methanol extract for a total volume of 600 µl. Lastly, the methanol was removed by centrifugal concentration and the remaining 2′-deoxynucleosides were resuspended in 1 ml of a 2 ng/ml solution of ddI internal standard in distilled water.

Instrumentation

LC/ESI–MS/MS analyses were performed using a Shimadzu HPLC system (Shimadzu) consisting of dual LC-10ADVP pumps and equipped with an SPD-10ADVP UV-visible detector interfaced with a Quattro Ultima triple stage quadrupole mass spectrometer (Micromass, Manchester, UK). The LC column was eluted over a gradient that began at a ratio of 15% methanol to 85% water and was changed to 80% methanol to 20% water over a period of 10 min. The 80:20 conditions were held for 10 min, and then returned to the original starting conditions, 15:85, which was held for the remaining period of 8 min. The total run time was 28 min during which the sample components were delivered to the mass spectrometer by electrospray. Sample injection volumes of 50 µl each were injected by a Shimadzu SIL-10ADVP autoinjector, separated on a Shim-pack FC-ODS, 150 × 4.6 mm column (Shimadzu) and eluted at a flow rate of 0.5 ml/min. Mass spectral analyses were carried out in positive ion mode with nitrogen as the nebulizing gas. The ion source temperature was 130°C, the desolvation temperature was 380°C, and the cone voltage was operated at a constant 35 V. Nitrogen gas was also used as the desolvation gas (700 L/h) and cone gas (35 L/h) and argon was used as the collision gas at a collision cell pressure of 1.5×10^{-3} mBar. Positive ions were acquired in MRM mode and the strategy was designed to detect the neutral loss of 2′-deoxyribose from positively ionized 2′-deoxynucleoside adducts by monitoring the samples transmitting their $[M + H]^+ > [M + H - 116]^+$ transitions as summarized in Fig. 1. For each DNA sample, from smoker and nonsmoker, a total of 374 MRM transitions were monitored over the range from transition *m/z* 228.8 > 112.8 through transition *m/z* 602.8 > 486.8. For each 50 µl sample injection, a total of 32 channels were monitored simultaneously, with one channel per injection always reserved to monitor the ddI internal standard at transition *m/z* 236.8 > 136.8. By using this strategy, each sample was injected 12 times to complete the monitoring of transitions from *m/z* 228.8 to 602.8.

The identification of specific target adducts N^2-ethyl-dG, N^2-methyl-dG, ϵdA, 1,N^2-PdG_1, and 1,N^2-PdG_2 were performed under the same LC/ESI–MS/MS conditions as above, except that the flow rate was 0.4 ml/min and the mobile phase was 98% water and 2% methanol, increased linearly to 60% water and 40% methanol over a period of 40 min, further increased to 20% water and 80% methanol for 5 min, and then returned to the original starting conditions of 98% water and 2% methanol for a total run time of 60 min. These conditions were used for unambiguous identification of some adducts. The MRM transitions monitored were as follows: [U-$^{15}N_5$]-1,N^2-PdG_1, [U-$^{15}N_5$]-1,N^2-PdG_2, *m/z* 342.8 > 226.8; 1,N^2-PdG_1, 1,N^2-PdG_2, *m/z* 337.8 > 221.8; [U-$^{15}N_5$]-N^2-ethyl-dG, *m/z* 300.8 > 184.8; N^2-ethyl-dG *m/z* 295.8 > 179.8; 8-oxo-dG, *m/z* 283.8 > 167.8; N^2-methyl-dG, *m/z* 281.8 > 165.8; and ϵdA, *m/z* 275.8 > 159.8.

Data processing

Data processing was performed in three stages. First, putative DNA adduct peaks were integrated using MassLynx 4.0 Global Mass–Informatics software. The program settings for integration were optimized such that automatic noise measurement was set to on, with mean smoothing enabled. Window size (scans) were set to ± 3, the number of smooths set to 3, and a threshold peak detect area of 500 (absolute area) was employed. In stage two, peak integration peak data were transferred to a Microsoft Excel spreadsheet, normalized based on the quantity of internal standard, ddI, detected for each injection, and manually screened for 2′-deoxynucleoside artifacts as per the information given in Table 1. In stage three, chromatograms for each $[M + H]^+ > [M + H - 116]^+$ transition, from *m/z* 228.8 to *m/z* 602.8, were individually analyzed to identify and eliminate DNA adduct isotope peaks. Such peaks occur due to a "carry-over" effect, whereby a putative DNA adduct peak detected at a specific retention time and transition, T, may also be detected at the same retention

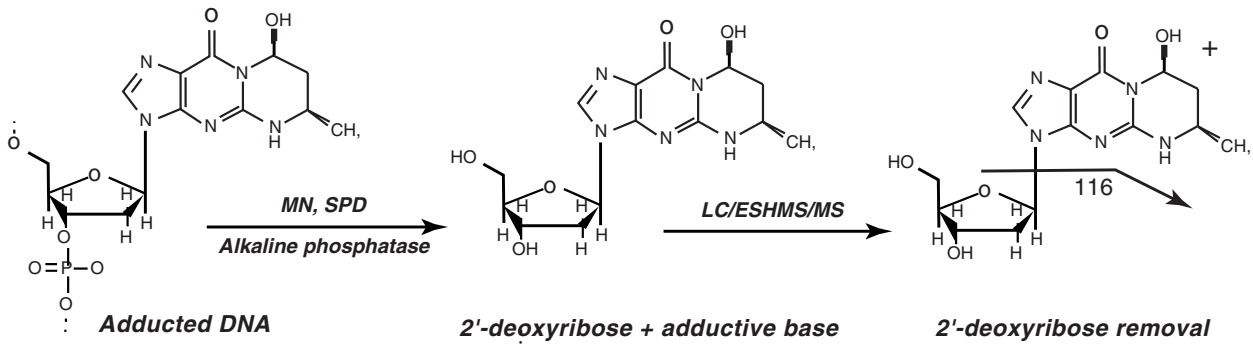

FIG. 1. Generalized depiction of the process for detecting DNA adducts by LC/ESI–MS/MS. After purification from lung tissue, DNA is digested to produce 2′-deoxyribose with target adducted bases attached. In the collision cell of the MS, the bond between 2′-deoxyribose and the target adducted base is broken and a proton is transferred from 2′-deoxyribose to the base. This results in the production of a protonated adducted base ion. The signal is transmitted to the detection system and recorded during sample monitoring in MRM mode transmitting the $[M + H]^+ > [M + H - 116]^+$ transition. In the above scheme, 1,N^2-propano-dG_1 is used as an example of a DNA adduct.

TABLE 1. THE ARTIFACTUAL POSITIVELY IONIZED 2′-DEOXYNUCLEOSIDES THAT WERE SCREENED OUT DURING STAGE I OF DATA ANALYSIS BASED UPON MASS TO CHARGE RATIO, *M/Z*

dN[a]	*M.W.*[b]	*R/T range*[c]	$+H^+$	$+NH_4^+$	$+Na^+$	$+K^+$	*Dimer*$+H^+$
dC	227.1	4.6–4.7	228.1	245.1	250.1	266.1	455.2
dT	242.1	8.6–8.7	243.1	260.1	265.1	281.1	485.1
dA	251.1	11.4–11.5	252.1	269.1	274.1	290.1	503.2
dG	267.1	6.6–6.9	268.1	285.1	290.1	306.1	535.2
5-methyl-dC	241.1	5.9–6.3	242.1	259.1	264.1	280.1	483.1

Values given as *m/z* unless otherwise indicated.

[a]2′-Deoxynucleosides: 2′-deoxycytidine; 2′-deoxythymidine; 2′-deoxyadenosine; 2′-deoxyguanosine.

[b]Molecular weight.

[c]Corresponding artifacts are detected within this HPLC retention time (R/T) range, postdigestion; units are in minutes.

time in subsequent transitions, T+1, T+2, etc. After stage three, data were used in the final analysis.

RESULTS

Figure 2 represents the final DNA adduct analysis organized as an adductome map. In the final analysis, a bubble-type chart was created whereby the x-axis represents the HPLC column retention time of the putative adduct, the y-axis represents the mass to charge ratio of the putative adduct, and the size of the bubble represents the putative adduct peak integration area normalized by the internal standard peak integration area, which is referred to hereafter as the area response. Charts from smoker and nonsmoker DNA were created and overlayed and the bubble size was standardized so that direct comparisons could be made between samples. In the final analysis, artifacts arising from the detection of positively ionized 2′-deoxynucleosides, their salts, and dimers were eliminated in stage two of data processing (Table 1). In mammalian DNA, 3%–5% of the cytosine residues are present as 5-methylcytosine (20) and 5-methyl-dC was also therefore included in the artifact elimination steps of stage two of the screening process. Artifacts arising from the detection of putative adduct isotopes were eliminated in stage three. In the final analysis, 776 and 675 putative DNA adducts were detected from the lung tissue DNA of a nonsmoker and smoker, respectively.

As shown in Fig. 2, putative DNA adducts were detected over the entire *m/z* range, from 228.8 to 602.8 through 28 min. During the first 10 min of elution, putative adducts generally occurred grouped in discreet retention time zones across the full *m/z* range, at approximately 3.3 ± 0.1, 4.5 ± 0.2, 5.5 ± 0.2, 6.9 ± 0.1, and 8.8 ± 0.2 min; indicated by the arrows in Fig. 2. By far the most active zone revealed by the final analysis—defined by large numbers of putative adducts that possessed the highest area response values—was detected between 3 and 15 min for putative adducts with *m/z* approximately less than 400 (indicated in Fig. 2 as zone A). In fact, of the 50 putative adducts with the largest area response

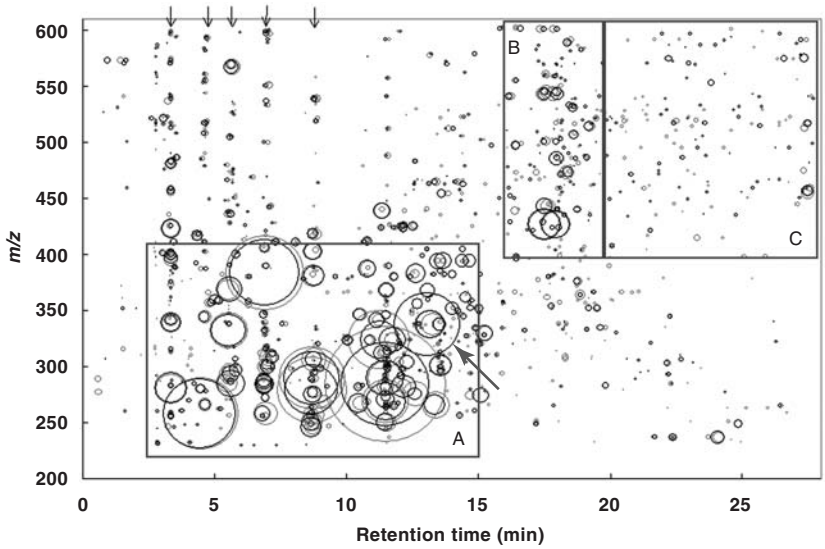

FIG. 2. Adductome map of putative DNA adducts detected in human lung tissue from a nonsmoker (*light circles*) and a smoker (*dark circles*). The neutral loss of 2′-deoxyribose from positively ionized 2′-deoxynucleoside putative adducts was analyzed by LC/ESI–MS/MS in MRM mode transmitting the $[M + H]^+ > [M + H - 116]^+$ transition over a total of 374 transitions in the mass range from *m/z* 228.8 to *m/z* 602.8. *Boxes A* through *C* define zones of activity that are discussed in the text. The *arrow* indicates the presence of a large putative adduct detected in the DNA of the smoker that was 4.8 times larger than in the DNA of the nonsmoker.

values detected from both tissue samples, 45 were detected in zone A. The exceptions were two pairs of unidentified putative adducts from each lung DNA sample that each occurred at *m/z* 426.8 in zone B plus an unidentified adduct at m/z 422.8 in the smoker. In zone B, a smaller active zone between 16 and 20 min, the largest molecular-sized putative adducts with the highest area response values were detected and these putative adducts likely represent less polar, bulky adducts. Indeed, due to their relatively high area response values, we are interested to investigate further the identities of putative adducts in zone B. The latest-eluting putative adducts, retention times greater than 20 min, were mostly putative adducts of large molecular size, *m/z* greater than 400, and are indicated by zone C. Adducts detected in zone C were the least likely to be shared between the lung sample DNA of the smoker and nonsmoker.

A comparison of the 20 putative adducts with the largest area response values from the DNA of the nonsmoker and smoker is given in Table 2. Interestingly, the largest 11 putative adducts detected in each lung tissue sample were identical, but not in the same order of area response. Additionally, the area response values for matching putative adduct pairs were similar in many cases. The sum of the total area responses of the largest 20 putative adducts was more than 1.5 times the sum of the total area responses of the remaining 756 putative adducts in the case of the DNA from the nonsmoker, and was more than 1.2 times the sum of the total area responses of the remaining 655 adducts from the DNA of the smoker. The similarity between the largest 20 putative adducts was 75% and as mentioned, most of these putative adducts were detected in zone A.

Demonstration of the utility of the final analysis

The final analysis revealed that many of the putative adducts that occurred with the largest area response values also occurred to similar extents in the DNA from each lung tissue sample, regardless of whether the sample was from the smoker or nonsmoker. This is clearly indicated in Fig. 2 by examining the largest light and dark circles that share the same *m/z*, same approximate retention time and similar size, especially within zone A. Of the largest 200 putative adducts detected from the nonsmoker and smoker, 142 were considered to be identical after matching their *m/z* values and retention times (71% similarity). After matching these adduct pairs and calculating the coefficient of variation between each (pair number = 142), the average percent coefficient of variation was found to be ± 17.3%. Although the putative adducts with the largest area response values occurred to sim-

TABLE 2. A COMPARISON OF THE LARGEST 20 PUTATIVE DNA ADDUCTS, BASED ON AREA RESPONSE AND ORGANIZED BY *M/Z*, IN HUMAN LUNG DNA FROM TWO INDIVIDUALS

Nonsmoker			*Smoker*		
m/z	*R/T*[a] *(min)*	*Area response*[b]	*m/z*	*R/T (min)*	*Area response*
257.8	4.47	25.3	257.8	4.43	24.4
278.8	8.72	21.8	278.8	8.68	13.3
280.8	3.33	4.0	280.8	3.34	5.4
283.8	11.50	66.9	283.8	11.46	35.2
289.8	8.70	19.9	289.8	8.68	14.4
323.8	11.25	17.0	323.8	11.27	7.3
331.8	5.55	6.7	331.8	5.52	5.5
337.8	13.12	4.2	337.8	13.08	20.0
383.8	6.91	28.4	383.8	6.89	22.5
426.8	17.52	4.7	426.8	17.52	5.1
426.8[c]	17.92	3.9	426.8	17.92	4.1
249.8	11.52	1.8	245.8	8.64	2.3
256.8	8.77	2.1	265.8	13.36	2.3
257.8	6.93	3.0	266.8	10.45	2.0
265.8	13.38	3.7	281.8	12.18	2.9
275.8	12.62	3.4	283.8	6.87	2.0
284.8	5.50	2.0	284.8	5.61	3.9
300.8	13.57	2.6	300.8	13.57	2.3
305.8	8.79	2.8	323.8	11.73	3.4
337.8	13.27	2.6	337.8	13.19	4.0

[a]HPLC column retention time.

[b]The area response is equal to the putative DNA adduct HPLC chromatogram peak integration area normalized by the internal standard HPLC chromatogram peak integration area, ddI.

[c]The largest 11 adducts from each lung sample were identical, but not in the same order, and are indicated above the bar.

ilar extents in the DNA of the smoker and nonsmoker, four cases of large differences were also revealed by the final analysis. In those cases, the area response values of a putative adduct from the DNA of the smoker exceeded by more than four times the area response of its counterpart from the nonsmoker. There was no case, however, where the reverse was true. All four putative adducts were detected in zone A and three shared *m/z* 393.8 and were unidentified. The last putative adduct was the fourth largest putative adduct detected overall from the DNA of the smoker, *m/z* 337.8, retention time equal to 13.08 min (Table 2), and it was 4.8 times greater than its counterpart in the nonsmoker DNA. In Figure 2, this putative adduct is indicated by the blue arrow.

As shown in Figure 3 in an expansion of an area of zone A, Fig. 2 of the final analysis, the presence of three pairs of putative adducts at *m/z* 337.8 were revealed. After consulting the literature, it was determined that one or two pairs of these putative adducts might be a candidate for the stereoisomers of the DNA adducts 1,N^2-propano-dG, 1,N^2-PdG_1, and/or 1,N^2-PdG_2, based on their *m/z* value of 337.8. Also indicated by Fig. 3, all three pairs of putative adducts were detected with greater area response values in the DNA of the smoker. Considering these results from the final analysis, standards of [U-$^{15}N_5$]-1,N^2-PdG_1 and [U-$^{15}N_5$]-1,N^2-PdG_2 were synthesized, spiked into postdigestion lung DNA samples and reanalyzed by LC/ESI–MS/MS under higher resolution LC conditions. The identities of two pairs of putative adducts appearing in the final analysis were unambiguously determined to be 1,N^2-PdG_1 and 1,N^2-PdG_2 by this stable isotope dilution technique, as indicated in Figure 4. Although the large peak was unidentified, recent analyses of experimental animal tissue DNA and human DNA samples (T. Matsuda, unpublished data) indicate that this peak is detected consistently and is always greater in size when compared to peaks of 1,N^2-PdG_1 and 1,N^2-PdG_2. Five smaller peaks were further resolved to elute just prior to the large peak by this LC separation gradient (Fig. 4B), and we postulate that the large putative adduct peak detected in the final analysis represents a group of DNA adducts, of regio- and stereoisomers of the 1,N^2-propano-dG-type adducts, all with molecular weights of 337. Indeed, four stereoisomers of 1,N^2-propano-dG adducts have been shown before (6) and in extensive studies detailing new adducts of acetaldehyde, crotonaldehyde, and related compounds, Wang *et al*. (16–18) characterized the DNA adduct N^2-(3-hydroxybutylidene)-dG, molecular weight equal to 337, and demonstrated at least four isomers. These isomers were stable in DNA and were formed in greater amounts than either 1,N^2-PdG_1 or 1,N^2-PdG_2, and they discussed the possibility that this might be true in human DNA (11).

Also illustrated in Fig. 3 are examples of (a) eight unidentified putative adduct pairs from zone A that were detected with greater area responses in the DNA of the smoker (with one exception); (b) one large unidentified putative adduct that was unique to the DNA of the smoker, *m/z* 367.8; and (c) one unambiguously identified adduct, ϵdA, *m/z* 275.8. Indeed, in addition to adducts of 1,N^2-propano-dG, we also assayed for the presence of three other adduct types in lung DNA that are thought to arise from endogenous or exogenous origins or both. Authentic standards of N^2-ethyl-dG, including [U-$^{15}N_5$]-N^2ethyl-dG, N^2-methyl-dG, and ϵdA were analyzed by LC/ESI–MS/MS with samples of lung DNA, or, in the case of [U-$^{15}N_5$]-N^2ethyl-dG, was spiked into postdigested lung DNA samples. N^2-ethyl-dG and ϵdA were detected and the four adducts that were positively identified in this study are summarized in Table 3.

DISCUSSION

The presence of DNA adducts in lung tissue or in any tissue is affected by a variety of temporal, genetic, and exposure factors that make for difficult analysis and results interpretation. However, the continual development of creative ways to approach and analyze DNA adducts may lead to new insights on their formation and roles in cancer and aging. In the final analysis described in this paper, 778 and 677 putative adducts were detected from the lung tissue DNA of a nonsmoker and smoker, respectively. These DNA adduct levels and types reflect previous long-term and recent exposures,

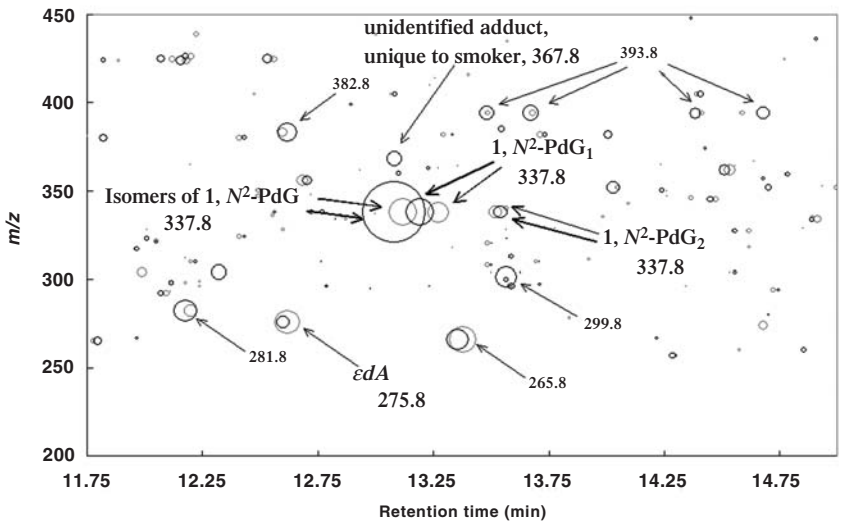

FIG. 3. Inset of an area of Zone A from the adductome map given in Fig. 1. Putative DNA adducts detected in human lung from a nonsmoker (*light circles*) and smoker (*dark circles*). Details are described in the text.

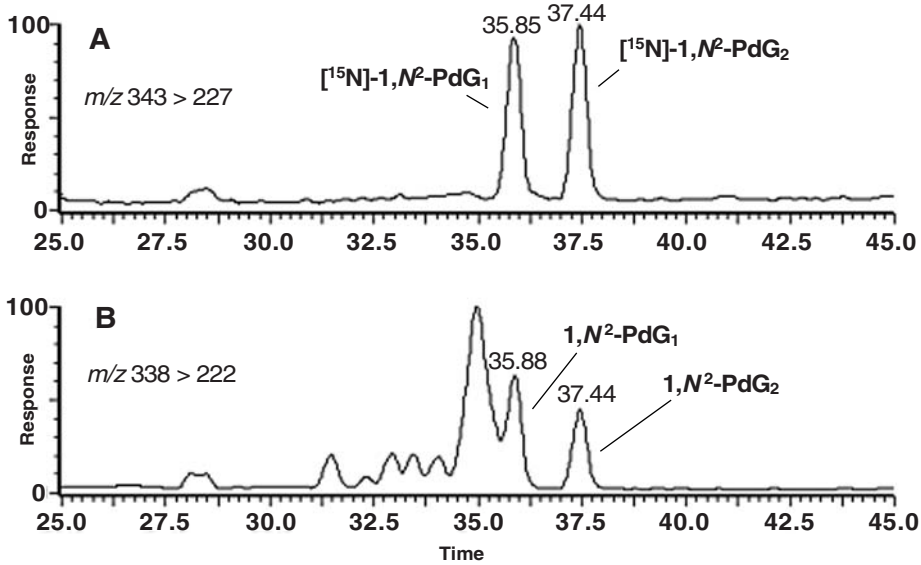

FIG. 4. LC/ESI–MS/MS detection of 1,N^2-propano-dG adducts in DNA extracted from human lung tissue. (**A**) Stable isotope internal standards [$^{15}N_5$]-1,N^2-PdG_1 and [$^{15}N_5$]-1,N^2-PdG_2 that were spiked into lung DNA samples and monitored at transition *m/z* 343 > 227. (**B**) Detection of 1,N^2-PdG_1 and 1,N^2-PdG_2 in lung DNA, monitored at transition *m/z* 338 > 222. The LC retention times are indicated above the peaks in minutes.

differences in metabolism and absorption, DNA repair mechanisms, and health status. However, even considering these factors, the final analysis indicated that there were putative adducts that were highly conserved among individuals or at least among lung tissue. The 25 largest occurring putative adducts were 75% similar and the largest occurring 13 adducts were identical in each individual, and in many cases they also occurred with similar area response values.

Most of the adducts with the largest area response values occurred in zone A, which was defined as a zone of high adduct activity and also represented a zone of high adduct conservation. Zones B and C were composed of high molecular weight adducts and were less conserved, with zone C showing very little adduct conservation between the two individuals (Fig. 2). To identify those zones where adduct formation is occurring at the greatest rate—or where slower repair or slower programmed cell death are occurring, for example—and then to attach unique identifiers to these adducts and perform correlation analyses, may result in the determination of whether certain adducts are correlated with exposure to tobacco smoke, or correlated with other factors such as age, sex, ethnicity, genetics, or disease state for example. Indeed, the development of the adductome mapping technique described in this report may enable us to begin to perform these types of investigations.

As mentioned, a key to expanding the power of the final analysis is to begin to assign identities to putative adducts. The LC/ESI–MS/MS was operated in positive ion mode; therefore, if the molecular weight of a known adduct is shown to be approximately equal to the *m/z* value of a putative adduct minus one, $[M + H]^+ - 1$, a positive match may be made, when taking into consideration other factors. However, this approach requires future validation. For illustrative purposes we include the following example: in both DNA samples, from the nonsmoker and smoker, the putative adducts that were detected with the largest area response values were identical, at *m/z* 283.8, average retention time equal to 11.48 ± 0.02 min and area response equal to 51.1 ± 15.9 (Fig. 2 and Table 2). It is known that adducts methylated at the N^7-position of dG are the most commonly occurring adducts in DNA, accounting for over 70% of all methylated adducts (19). Considering this, and based on the *m/z* of this putative adduct, we might weakly assign a tentative identity of N^7-methyl-dG to this putative adduct, which has a molecular weight of 283.2. The heavily studied oxidative lesion 8-oxo-dG is also of molecular weight 283.2. However, the putative adduct in ques-

TABLE 3. DNA ADDUCTS POSITIVELY IDENTIFIED BY LC/ESI–MS/MS DETECTION IN DNA EXTRACTED FROM HUMAN LUNG TISSUE

m/z	*R/T*[a] *range (min)*	*Area response*[b]	*Adduct*	*Method of detection*
337.8	13.19–13.27	3.34 ± 0.72	1,N^2-PdG_1	Stable isotope dilution
337.8	13.52–13.54	0.93 ± 0.02	1,N^2-PdG_2	Stable isotope dilution
295.8	13.21–13.23	0.02 ± 0.01	N^2-Ethyl-dG	Stable isotope dilution
275.8	12.60–12.62	2.15 ± 1.27	ϵdA	Comparison to authentic ϵdA standard

[a]HPLC column retention time.
[b]Area response ± the coefficient of variation.

tion and another putative adduct detected at transition 283.8 > 167.8 were determined not to be 8-oxo-dG based on retention time data after further LC/ESI–MS/MS analysis of an 8-oxo-dG authentic standard (data not shown).

Of course, as was shown in this paper, the best-case scenario is to confirm adductome putative adduct identities by unambiguous identification through stable isotope dilution and comparison to authentic standards. 1,N^2-PdG_1, 1,N^2-PdG_2, N^2-ethyl-dG, and ϵdA were confirmed in both DNA samples extracted from human lung. In the case of the smoker, 1,N^2-PdG_1, 1,N^2-PdG_2, and N^2-ethyl-dG, were detected with greater area response values, whereas ϵdA was detected with a greater area response value in the nonsmoker; the case of ϵdA is clearly indicated in Fig. 3. It may be worth mentioning that etheno-DNA adducts in human lung detected by the sensitive ^{32}P-post labeling assay were found not to be influenced by smoking behavior in at least one study (8). The final analysis also revealed the presence of a large putative adduct in the DNA of the smoker that was 4.8 times larger than its counterpart in the nonsmoker and this putative adduct may represent a group of 1,N^2-propano-related isomers formed by reactions involving acetaldehyde, crotonaldehyde, and other similar compounds. As is known, acetaldehyde and crotonaldehyde are constituents of tobacco smoke and acetaldehyde concentrations (μg/cigarette) may be greater than polycyclic aromatic hydrocarbons or tobacco-specific nitrosamines by more than 1,000 times (3, 10).

Although we are careful not to draw many conclusions from a sample set of two individuals, it was interesting that putative adducts from the lung DNA of the smoker were detected with larger area response values in the cases of key adducts implicated in exposure to tobacco smoke. Future analysis with lung tissue DNA from a larger pool of individuals may provide the necessary information to establish if there is a relationship between these adducts and tobacco smoke. Herein we are simply demonstrating that this methodology may provide us with a novel set of tools to perform more comprehensive analyses in the future.

This report describes the adductome approach to detect DNA damage: a novel method to analyze DNA adducts. Our ability to analyze large numbers of DNA adducts have until now been constrained by a variety of factors. With the tools to analyze large numbers of adducts combined with the ability to match their identities, the methodology described in this report will allow for more in-depth analyses that may span tissue types, exposure types, genotypes, etc., and will aid in addressing such issues as interindividual and intertissue DNA adduct variation. The methodology will be subjected to continual refinement and development as part of a wider plan to organize the rapidly expanding literature in regard to oxidative DNA adducts and others through the creation of a DNA adduct database at Kyoto University. Our aims include engaging in an exhaustive search to organize all known types of DNA adducts and to utilize this information in the DNA adduct monitoring methodology described in this report.

ACKNOWLEDGMENTS

This work was supported in part by grants-in-aid for cancer research from the Japanese Ministry of Health, Labor, and Welfare, for scientific research (15681002) from MEXT, Japan, from NEDO, Japan and by the Japan Society for the Promotion of Science (JSPS).

ABBREVIATIONS

AA, acetaldehyde; dA, 2′-deoxyadenosine; ddI, dideoxyinosine; dC, 2′-deoxycytidine; dG, 2′-deoxyguanosine; DMSO, dimethyl sulfoxide; dN, 2′-deoxynucleoside; dT, 2′-deoxythymidine; ϵdA, 1,N^6-etheno-2′-deoxyadenosine; LC/ESI–MS/MS, liquid chromatography/electrospray ionization–tandem mass spectrometry; malonaldehyde-dG, pyrimido[1,2α]purine-10(3H)one-2′-deoxyguanosine; MN, micrococcal nuclease; MRM, multiple reaction ion monitoring mode; N^2-ethyl-dG, N^2-ethyl-2′-deoxyguanosine; N^2-methyl-dG, N^2-methyl-2′-deoxyguanosine; 1,N^2-PdG_1, α-*S*-methyl-γ-hydroxy-1,N^2-propano-2′-deoxyguanosine; 1,N^2-PdG_2, α-*R*-methyl-γ-hydroxy-1,N^2-propano-2′-deoxyguanosine; R/T, retention time; SPD, bovine spleen phosphodiesterase II; 8-oxo-dG, 8-oxo-7,8-dihydro-2′-deoxyguanosine.

REFERENCES

1. Barbin A, Ohgaki H, Nakamura J, Kurrer M, Kleihues P, and Swenberg JA. Endogenous deoxyribonucleic acid (DNA) damage in human tissues: a comparison of ethenobases with aldehydic DNA lesions. *Cancer Epidemiol Biomarkers Prev* 12: 1241–1247, 2003.
2. Beland FA, Churchwell MI, Von Tungeln LS, Chen S, Fu PP, Culp SJ, Schoket B, Gyorffy E, Minárovits J, Poirier MC, Bowman ED, Weston A, and Doerge DR. High-performance liquid chromatography electrospray ionization tandem mass spectrometry for the detection and quantitation of benzo[*a*]pyrene-DNA adducts. *Chem Res Toxicol* 18: 1306–1315, 2005.
3. Chepiga TA, Morton MJ, Murphy PA, Avalos JT, Bombick BR, Doolittle DJ, Borgerding MF, and Swauger JE. A comparison of the mainstream smoke chemistry and mutagenicity of a representative sample of the US cigarette market with two Kentucky reference cigarettes (K1R4F and K1R5F). *Food Chem Toxicol* 38: 949–962, 2000.
4. Churchwell MI, Beland FA, and Doerge DA. Quantification of multiple DNA adducts formed through oxidative stress using liquid chromatography and electrospray tandem mass spectrometry. *Chem Res Toxicol* 15: 1295–1301, 2002.
5. Doerge DR, Churchwell MI, Fang J-L, and Beland FA. Quantification of etheno-DNA adducts using liquid chromatography, on-line sample processing, and electrospray tandem mass spectrometry. *Chem Res Toxicol* 13: 1259–1264, 2000.
6. Eder E and Hoffman C. Identification and characterization of deoxyguanosine-crotonaldehyde adducts. Formation of 7,8 cyclic adducts and 1,N^2,7,8 bis-cyclic adducts. *Chem Res Toxicol* 5: 802–808, 1992.
7. Esaka Y, Inagaki S, and Goto M. Separation procedures capable of revealing DNA adducts. *J Chromatog B*, 797: 321–329, 2003.

8. Godschalk R, Nair J, van Schooten FJ, Risch A, Drings P, Kayser K, Dienemann H, and Bartsch H. Comparison of multiple DNA adduct types in tumor adjacent human lung tissue: effect of cigarette smoking. *Carcinogenesis* 23: 2081–2086, 2002.
9. Kadlubar FF, Anderson KE, Häussermann S, Lang NP, Barone GW, Thompson PA, MacLeod SL, Chou MW, Mikhailova M, Plastaras J, Marnett LJ, Nair J, Velic I, and Bartsch H. Comparison of DNA adduct levels associated with oxidative stress in human pancreas. *Mutat Res* 405: 125–133, 1998.
10. Lao Y and Hecht SS. Synthesis and properties of an acetaldehyde-derived oligonucleotide interstrand cross-link. *Chem Res Toxicol* 18: 711–721, 2005.
11. Thiele GM, Worrall S, Tuma DJ, Klassen LW, Wyatt TA, and Nagata N. The chemistry and biological effects of malonaldehyde-acetaldehyde adducts. *Alcohol Clin Exp Res* 25: 218–224, 2001.
12. Thomson NM, Mijal RS, Ziegel R, Fleischer NL, Pegg AE, Tretyakova NY, and Peterson LA. Development of a quantitative liquid chromatography/electrospray mass spectrometric assay for a mutagenic tobacco specific nitrosamine-derived DNA adduct, O^6-[4-oxo-4-(3-pyridyl) butyl]-2′-deoxyguanosine. *Chem Res Toxicol* 17: 1600–1606, 2004.
13. Turesky RJ and Vouros P. Formation and analysis of heterocyclic aromatic amine-DNA adducts *in vitro* and *in vivo*. *J Chromatog B* 802: 155–166, 2004.
14. Ricicki EM, Soglia JR, Teitel C, Kane R, Kadlubar F, and Vouros P. Detection and quantification of *N*-(deoxyguanosin-8-yl)-4-aminobiphenyl adducts in human pancreas tissue using capillary liquid chromatography–microelectrospray mass spectrometry. *Chem Res Toxicol* 18: 692–699, 2005.
15. Sako M, Kawada H, and Hirota K. A convenient method for the preparation of N^2-ethylguanine nucleosides and nucleotides. *J Org Chem* 64: 5719–5721, 1999.
16. Wang M, McIntee EJ, Cheng G, Shi Y, Villalta PW, and Hecht SS. A Schiff base is a major adduct of crotonaldehyde. *Chem Res Toxicol* 14: 423–430, 2001.
17. Wang M, McIntee EJ, Cheng G, Shi Y, Villalta PW, and Hecht SS. Reactions of 2,6-dimethyl-1,3-dioxane-4-ol (aldoxane) with deoxyguanosine and DNA. *Chem Res Toxicol* 14: 1025–1032, 2001.
18. Wang M, McIntee EJ, Shi Y, Cheng G, Upadhyaya P, Villalta PW, and Hecht SS. Reactions of α-acetoxy-*N*-nitrosopyrrolidne with deoxyguanosine and DNA. *Chem Res Toxicol* 14: 1435–1445, 2001.
19. YangY, Nikolic D, Swanson SM, and van Breemen RB. Quantitative determination of N^7-methylguanosine and O^6-methylguanosine in DNA by LC–UV–MS–MS. *Anal Chem* 74: 5376–5382, 2002.
20. Ziegel R, Shallop A, Upadhyaya P, Jones R, and Tretyakova N. Endogenous 5-methylcytosine protects neighboring guanines from N7 and O^6-methylation and O^6-pyridyloxobutylation by the tobacco carcinogen 4-(methylnitrosamino)-1-(3-pyridyl)-1-butanone. *Biochemistry* 43: 540–549, 2004.

Address reprint requests to:
Tomonari Matsuda
Department of Technology and Ecology
Graduate School of Global Environmental Studies
Kyoto University
Kyoto, Japan 606-8501

E-mail: matsuda@eden.env.kyoto-u.ac.jp

Date of first submission to ARS Central, December 1, 2005; date of acceptance, December 19, 2005.

This article has been cited by:

1. Stephen M. Rappaport, He Li, Hasmik Grigoryan, William E. Funk, Evan R. Williams. 2012. Adductomics: Characterizing exposures to reactive electrophiles. *Toxicology Letters* **213**:1, 83-90. [CrossRef]
2. Jean-Luc Ravanat. 2012. Chromatographic methods for the analysis of oxidatively damaged DNA. *Free Radical Research* 1-13. [CrossRef]
3. Sabine Plattner, Robert Erb, Florian Pitterl, Hendrik-Jan Brouwer, Herbert Oberacher. 2011. Formation and characterization of covalent guanosine adducts with electrochemistry—liquid chromatography–mass spectrometry. *Journal of Chromatography B* . [CrossRef]
4. Anthony M. Lynch, Jennifer C. Sasaki, Rosalie Elespuru, David Jacobson-Kram, Véronique Thybaud, Marlies De Boeck, Marilyn J. Aardema, Jiri Aubrecht, R. Daniel Benz, Stephen D. Dertinger, George R. Douglas, Paul A. White, Patricia A. Escobar, Albert Fornace, Masamitsu Honma, Russell T. Naven, James F. Rusling, Robert H. Schiestl, Richard M. Walmsley, Eiji Yamamura, Jan van Benthem, James H. Kim. 2011. New and emerging technologies for genetic toxicity testing. *Environmental and Molecular Mutagenesis* **52**:3, 205-223. [CrossRef]
5. Kyoko Kato, Eiji Yamamura, Masanobu Kawanishi, Takashi Yagi, Tomonari Matsuda, Akio Sugiyama, Yoshifumi Uno. 2011. Application of the DNA adductome approach to assess the DNA-damaging capability of in vitro micronucleus test-positive compounds. *Mutation Research/Genetic Toxicology and Environmental Mutagenesis* **721**:1, 21-26. [CrossRef]
6. Kuen-Yuh Wu, Su-Yin Chiang, Wei-Chung Shih, Chih-Chun Jean Huang, Ming-Feng Chen, James A. Swenberg. 2011. The application of mass spectrometry in molecular dosimetry: Ethylene oxide as an example. *Mass Spectrometry Reviews* n/a-n/a. [CrossRef]
7. Rajinder Singh, Friederike Teichert, Albrecht Seidel, Jonathan Roach, Rebecca Cordell, Mai-Kim Cheng, Heinrich Frank, William P. Steward, Margaret M. Manson, Peter B. Farmer. 2010. Development of a targeted adductomic method for the determination of polycyclic aromatic hydrocarbon DNA adducts using online column-switching liquid chromatography/tandem mass spectrometry. *Rapid Communications in Mass Spectrometry* **24**:16, 2329-2340. [CrossRef]
8. Hiroshi Nishida, Masanobu Kawanishi, Takeji Takamura-Enya, Takashi Yagi. 2008. Mutagenic specificity of N-acetoxy-3-aminobenzanthrone, a major metabolically activated form of 3-nitrobenzanthrone, in shuttle vector plasmids propagated in human cells. *Mutation Research/Genetic Toxicology and Environmental Mutagenesis* **654**:1, 82-87. [CrossRef]
9. Paul T. J. Scheepers. 2008. The use of biomarkers for improved retrospective exposure assessment in epidemiological studies: summary of an ECETOC workshop*. *Biomarkers* **13**:7-8, 734-748. [CrossRef]
10. Robert A. Kanaly, Saburo Matsui, Tomoyuki Hanaoka, Tomonari Matsuda. 2007. Application of the adductome approach to assess intertissue DNA damage variations in human lung and esophagus. *Mutation Research/Fundamental and Molecular Mechanisms of Mutagenesis* **625**:1-2, 83-93. [CrossRef]
11. Shana J Sturla. 2007. DNA adduct profiles: chemical approaches to addressing the biological impact of DNA damage from small molecules. *Current Opinion in Chemical Biology* **11**:3, 293-299. [CrossRef]
12. Antonysunil Adaikalakoteswari, Mohan Rema, Viswanathan Mohan, Muthuswamy Balasubramanyam. 2007. Oxidative DNA damage and augmentation of poly(ADP-ribose) polymerase/nuclear factor-kappa B signaling in patients with Type 2 diabetes and microangiopathy. *The International Journal of Biochemistry & Cell Biology* **39**:9, 1673-1684. [CrossRef]